npj | microgravity

Article

Published in cooperation with the Biodesign Institute at Arizona State University, with the support of NASA

https://doi.org/10.1038/s41526-026-00668-z

Growth and molecular responses of potato to lunar regolith simulants

Check for updates

David Handy, Anika Loeffler, Medora Knudson, Sydney Campbell, Pankaj Jaiswal, Jeffrey C. Anderson & Aymeric Goyer ✉

Long-duration lunar exploration will depend on bioregenerative life support systems capable of producing food on-site, making the viability of crop production in lunar regolith a critical research priority. We evaluated potato (*Solanum tuberosum* L.) as a candidate food crop by growing plants in five lunar regolith simulants (LRSs), with varying levels of vermicompost amendment, under controlled greenhouse conditions. Growth in unamended simulant severely restricted biomass, while addition of organic matter to LRS progressively restored yield. At low amendment levels, all LRS types reduced canopy size and tuber yield relative to a terrestrial soil control, with responses varying by simulant type. Whole-transcriptome profiling of leaves revealed that each simulant elicited a distinct pattern of gene expression changes, indicating that the type and intensity of regolith-induced stress is substrate-dependent. In contrast, tuber metabolite composition showed minimal deviation from control plants. Heavy metals, including Cu, Zn, and Al, were modestly elevated in tubers from certain LRS treatments, warranting continued monitoring in future studies. Collectively, our results indicate that potato can complete its life cycle and produce nutritionally acceptable tubers in LRS when supplemented with organic matter, while underscoring the need to better understand substrate-specific phytotoxicity to optimize crop production in early-stage lunar agriculture.

Establishing a permanent human presence on the Moon in the 2030s is the goal of NASA's Artemis missions[1]. This will require on-site sustainable and affordable food production to reduce resupply costs and increase mission success probabilities[2]. Regolith-based agriculture has been proposed as an in-situ method of supporting crops for food production. However, whether surface lunar regolith can be used as plant growth support needs to be verified to ensure adequate food production and food safety.

Lunar regolith falls into two categories: lunar mare and lunar highlands. The primary component in lunar mare regolith is basalt formed by lava flows during the volcanically active phase, while the geologically older, crater-filled lunar highlands primarily consist of ferroan anorthosite[3]. One of the most unique feature of lunar regolith compared to terrestrial soils is the presence of agglutinates, aggregate particles formed by micrometeorite impacts and comprised of nanophase iron, mineral fragments, and glass. These sharp nanoparticles may cause abrasive stress on exposed tissues, contributing to the overall stresses plants face in regolith-based agriculture. As genuine lunar regolith is not available for large-scale plant studies, different types of lunar regolith simulants (LRS) have been designed and manufactured and are commonly used for plant biology experimentation[4–6].

Potato (*Solanum tuberosum* L.) is an ideal clonally propagated food crop for space exploration because it provides more calories per land area than many other crops, it is nutritious, and it has a high satiety index. Potato is also a good model organism for plants that produce underground tubers because it has a large germplasm, sequenced genomes, and many publicly available large-scale omics datasets. However, we currently have limited knowledge of how potato might respond to lunar regolith and LRS as a growth substrate. Stunted and inadequate plant growth has been identified in various species grown in lunar and Martian regolith simulants[7,8]. In potato, the early experiments of Walkinshaw et al. using samples returned from Apollo missions were limited to evaluating the response of potato seedlings to lunar soil exposure[9]. The authors grew potato seedlings on mineral solution (Hutner's or Hoagland's) and abraded the leaves with a suspension of lunar soil material. In their report, the authors did not explicitly describe what the response was. It follows that we have limited knowledge about the adaptability of potato to grow on lunar regolith simulant and the underlying mechanisms of acclimation. Furthermore, we have limited knowledge of the chemistry of potato tubers produced on lunar regolith simulant and whether they are safe for consumption by space exploration crews. Seedlings of several plant species accumulated large amounts of aluminum, iron, and titanium when grown in lunar regolith

Department of Botany and Plant Pathology, Oregon State University, Corvallis, OR, USA. ✉e-mail: Aymeric.goyer@oregonstate.edu

from Apollo 14[10]. If these ions were to accumulate in potato tubers, they could have negative health effects on humans. In addition, potatoes produce glycoalkaloids that are toxic for humans if present at unsafe levels. Glycoalkaloids accumulate in stressed potato plants. It is therefore important to assess levels of these chemicals in tubers produced in lunar regolith simulants.

The objectives of this study were to (1) determine the viability of using organic amendments to remediate LRS, (2) assess differences in response to a variety of LRS types, and (3) characterize molecular responses of potato to LRS. Because previous studies reported that growth of different plant species is severely affected in 100% LRS and proposed a variety of organic amendments[11–13] to alleviate this issue, we aimed to identify a ratio of LRS/compost that supports sufficient potato plant growth for phenotypic characterization, but is also optimal to investigate the stress response to LRS. In addition, lunar regolith and LRS vary in their composition. Therefore, we tested whether potato responds similarly or differently to a variety of LRS types, i.e., mare or highland, mixed with compost by monitoring growth and physiology, quantifying biomass yield, and analyzing the potato leaf transcriptome and select leaf and tuber metabolites. Additionally, we analyzed various characteristics of the LRSs such as pH, electroconductivity (EC), heavy metal content, and microbial respiration pre- and post-plant growth to determine how the plants affected the soil environment. To our knowledge, this is the first report of the response of potato to LRS with fully-grown plants.

Methods

Chemicals

Chlorogenic acid, HPLC-grade acetonitrile, HPLC-grade methanol, and meta-phosphoric acid were from VWR (Radnor, PA, USA). L-Phenylalanine, L-tyrosine, ascorbic acid, solanine, chaconine, methoxamine, pyridine, and ribitol were from Millipore-Sigma (St. Louis, MO, USA). N-methyl-N-(trimethylsilyl) trifluoroacetamide with chlorotrimethylsilane was purchased from CovaChem (Loves Park, IL, USA).

Potato and growth substrate materials

Mini-tubers of Modoc, a red skin and white flesh potato variety, were obtained from CSS Farms, Colorado City, CO, USA (https://cssfarms.com/). In addition to its high yield and early maturing characteristics, we chose a colored skin variety because skin color is an important attribute for consumers' appeal for food[14], in this case, space explorers. Lunar regolith simulants LHS-1E and LMS-1E were purchased from the Exolith Lab (Orlando, FL, USA), and JSC-1A, OPRH4W30, and NUW-LHT-5M were obtained from NASA (Johnson Space Center Simulant Development Lab). JSC-1A and LMS-1E are lunar mare regolith simulants, OPRH4W30, LHS-1E, and NUW-LHT-5M are lunar highlands regolith simulants. OPRH4W30 was included because it is formulated to resemble lunar regolith found in the lunar south pole, where NASA has identified multiple regions as candidate landing sites for future lunar exploration missions[15]. JSC-1A is a NASA reference simulant[16], NUW-LHT-5M has better highland glass chemistry than OPRH4W30[17], and LHS-1E and LMS-1E are commercially available and could be obtained in larger quantities for studies like ours[18,19]. The Adkins-series sandy soil was collected from Hermiston, Oregon, USA (45.817318°N–119.294922°W), a region known for the highest potato yields in the world, and used as an optimal potato growth Earth control[20]. Vermicompost was sourced from Earthworm Castings (Green Bay, WI, USA) and was selected to mimic the use of waste plant matter as soil amendment in a bioregenerative life support system.

Growth conditions

Experiment 1: Determination of optimal LRS/compost ratio. Growth substrates were prepared by blending LMS-1E with vermicompost at 0%, 15%, and 30% (v/v), yielding a pure regolith control (100% LMS-1E) and two amended treatments containing 85% and 70% LMS-1E. Mixtures were prepared by combining 5% non-autoclaved vermicompost with 10% or 25% autoclaved vermicompost in 85% or 70% LMS-1E (volume ratios), respectively. We used a consistent amount of non-autoclaved vermicompost between batches to minimize potential confounding effects of microbial load. Adkins-series sandy soil mixed with vermicompost at equivalent ratios served as the terrestrial reference control.

As LRSs lack nitrogen and vermicompost would only provide a small portion of the nitrogen needed by the plants (see below), all treatments were supplemented with Osmocote Plus 15-9-12 slow-release fertilizer at 5.68 cm^3 per 1000 cm^3 of substrate to eliminate confounding effects of macronutrient deficiency. Our goal was to understand the effects of lunar regolith simulants on potato performance. Therefore, it was important to eliminate any potential confounding effects of soil nitrogen deficiency. We estimate that vermicompost, which contains 0.5% total N, 0.03% soluble, 0.47% insoluble according to the manufacturer, will provide ~0.18 g total N per 300 cm^3 pot, based on an 85/15 (v/v) ratio simulant/compost and assuming a density of 0.8 g per cm^3. Of compost total nitrogen, only ~10% is available to the plant[21], or ~0.018 g per 300 cm^3. Typically, one potato plant grown in the field for commercial production requires 5.6 g N per season (~ 200 kg N/ha, ~35,900 potato plants per hectare based on 30-cm plant spacing and 91-cm row spacing) (Table S1). Even if we assume that plants grown in pots in a greenhouse will produce a total biomass a 1/50th of that produced by plants grown in the field, plant-available nitrogen will still be suboptimal. The goal is to supply enough nitrogen in the growth media to prevent nitrogen deficiency in plant tissues, so that any response of the plants is independent of nitrogen stress. We also estimated the needs of potato plants for other macro- and micro-nutrients and the amounts that lunar regolith simulants might provide on a per pot basis based on the references listed in Table S1. Note that the estimated needs of potato plants are based on nutrient management recommendations for potatoes grown in the field where yields are expected to be higher than in pots and thus are likely overestimates. Nevertheless, they are useful to understand what nutrients might be deficient or in excess in lunar regolith simulants for optimal plant growth. Based on our calculations, lunar regolith simulants would not provide enough phosphorus and potassium for plants' needs, but an excess of iron, magnesium, manganese, and calcium. It should be noted that phosphorus availability to plants is highly dependent on pH and the presence of other elements such as iron, aluminum and calcium[22]. Iron, aluminum and calcium represent a large proportion of the total elemental composition of lunar regolith simulants and will be present in amounts much larger than needed by plants[6,23]. Therefore, the amount of phosphorus available to plants might be much smaller than these estimated numbers.

Modoc potato variety mini-tubers were planted on 2 August 2024 in 8.89 × 7.62 cm square pots (approximately 300 cm^3 substrate) lined with landscaping fabric (Greenhouse Megastore, Danville, IL, USA). Six treatments (two soil types × three compost ratios) were established with six replicated pots each. Some plants did not emerge, so the number of biological replicates varied between 3 and 6. Pots were arranged in a fixed randomized design under a PlantEye600 multispectral scanner (Phenospex, Heerlen, The Netherlands), with a border row included to minimize edge effects. Plants were maintained in an Oregon State University greenhouse at 22 °C day/18 °C night under natural light and irrigated with 40 mL reverse osmosis water every 2–3 days, increasing to daily irrigation as plants matured.

Canopy growth was monitored via PlantEye600 scans acquired every 12 hours for the first two weeks post-emergence (weeks 4 to 6 post-planting) until canopy overlap precluded individual plant discrimination. Measured traits included digital biomass, height, leaf area, leaf angle, hue, greenness, normalized difference vegetation index (NDVI), normalized pigment chlorophyll index (NPCI), and plant senescence reflectance index (PSRI). At 63 days after planting (DAP), photosynthetic parameters, including quantum yield, electrochromic shift, and non-photochemical quenching, and leaf pigment content were measured using a MultispeQ device (PhotosynQ Inc., East Lansing, MI, USA).

Plants were harvested at 74 DAP (15 October 2024) following confirmed tuber set. Roots and tubers were rinsed with tap water, and residual substrate was sieved to remove roots, stolons, and fertilizer pellets prior to

collection for post-growth chemical and microbial respiration analyses (see below). Above- and below-ground tissues were separated into shoots, roots, and tubers and weighed individually. Harvest index was calculated as the percentage of edible biomass relative to total plant biomass (100 × tuber mass/total biomass). Leaves and tubers were flash frozen in liquid nitrogen, lyophilized for 48 h in a Virtis Benchtop 4.0 K XL freeze-dryer (SP Industries Inc., Warminster, PA, USA), and ground to powder with mortar and pestle for elemental nutrient analysis.

Experiment 2: Effect of various lunar regolith simulant types. Adkins-series sandy soil and five LRSs (LHS-1E, LMS-1E, JSC-1A, OPRH4W30, and NUW-LHT-5M) were each amended with vermicompost at 5% (v/v). This amendment level was selected to provide sufficient biomass for tuber yield quantification and downstream nucleic acid and metabolite extractions, while maintaining a degree of substrate stress sufficient to elicit a detectable plant response, consistent with findings from Experiment 1, in which unamended LRS precluded quantifiable tuber production. A 5% organic matter fraction was also considered representative of early-stage organic matter incorporation in a bioregenerative life support system.

Mini-tubers were allowed to sprout at room temperature and planted once sprouts reached approximately 2 cm in length. One tuber per pot was planted in 8.89 × 7.62 cm square pots lined with landscaping fabric, with five biological replicates per soil type ($n = 30$ plants total) arranged in a completely randomized design. Canopy development was monitored via PlantEye600 scans (Phenospex, Heerlen, The Netherlands) acquired every 12 h from 5 May through 9 June (35 DAP), after which plant size exceeded the spacing required for individual plant discrimination.

Upper canopy leaf samples were collected at 39 DAP and immediately flash-frozen in liquid nitrogen for RNA-seq and metabolite analyses. Leaf tissue was collected prior to final harvest to avoid confounding effects of senescence on transcriptomic and metabolomic profiles. Leaves were not collected from plants grown in NUW-LHT-5M due to severely stunted growth and absence of harvestable leaf tissue. At 59 DAP, tubers were harvested, weighed, flash-frozen in liquid nitrogen, lyophilized, and ground to a fine powder using a mortar and pestle for metabolite analysis (see untargeted and targeted metabolite analysis sections below). Senesced shoot tissue was not collected for analysis across any treatment.

Soil and tissue analyses

Soil physicochemical properties, including EC, pH, moisture, microbial respiration, organic matter content, and elemental nutrient content (inclusive of heavy metals), and elemental composition of leaf and tuber tissues were determined by the Oregon State University Soil Health Lab. Pre-growth substrate samples were retained from each LRS prior to planting for baseline comparison. In Experiment 1, soil and freeze-dried tissue samples were pooled across three biological replicates per treatment; in Experiment 2, four biological replicates were analyzed independently. Additionally, in Experiment 2, a sample of each regolith mixed with vermicompost was taken before planting to serve as a pre-growth control. Soil EC and pH were measured in 1:1 (w/v) substrate-to-deionized water suspensions using a Hanna HI5522 instrument equipped with either a pH/temperature or EC probe as appropriate (Hanna Instruments, Woonsocket, RI, USA). Microbial respiration was assessed by CO_2 burst test, in which wet substrate was incubated in a sealed vessel at 23 °C for up to 96 h, with CO_2 measured at 0, 24, and 96 h using a Picarro isotopic CO_2 analyzer (Picarro, Inc., Santa Clara, CA, USA).

Elemental analysis differed between experiments to reflect their respective objectives. In Experiment 1, total elemental content of substrate (500 mg) and plant tissue (250 mg) was determined by nitric acid digestion followed by microwave-assisted extraction (Anton Paar, Ashland, VA, USA) and Inductively Coupled Plasma Optical Emission Spectroscopy (ICP-OES) quantification (Agilent 5110, Agilent Technologies, Santa Clara, CA, USA), targeting Al, As, Cd, Co, Cr, Cu, Ni, Pb, and Zn. As this method captures total rather than bioavailable elemental fractions, tissue analysis is more informative than soil analysis under this protocol, and results from soil elemental measurements in Experiment 1 should be interpreted accordingly. In Experiment 2, bio-extractable soil nutrients were assessed using Mehlich-3 solution (20 g L^{-1} NH_4NO_3, 5.556 mg mL^{-1} NH_4F, 0.372 mg mL^{-1} EDTA, 11.5 mL L^{-1} glacial acetic acid, 0.82 mL L^{-1} HNO_3; 20 mL per 2 g sample, shaken for 5 min, filtered) and quantified by ICP-OES for Al, Ca, Cu, Fe, K, Mg, Mn, P, and Zn elements selected for their relevance to plant nutrition and their potential phytotoxicity at elevated concentrations. Plant tissue in Experiment 2 was digested and analyzed by ICP-OES as described for Experiment 1.

Untargeted metabolite analysis using gas chromatography-mass spectrometry (GC-MS)

Tissue extracts were analyzed by GC-MS as previously described[24]. Briefly, 50 mg of dried tissue was extracted using a water:-methanol:chloroform (1:2.5:1) solution with ribitol (40 µg mL^{-1}) as an internal standard. Extracts were centrifuged to remove cellular debris, then phase separated to isolate aqueous compounds. Fifty µL aliquots were frozen and lyophilized then stored at −80 °C. Samples were derivatized by resuspension of lyophilized material into 20 µL methoxamine HCl (30 mg mL^{-1}) dissolved in pyridine and incubating the sample at 37 °C for 90 min with shaking. Then, 40 µL of N-methyl-N-(trimethylsilyl) trifluoroacetamide with 1% chlorotrimethylsilane was added to each sample followed by a 30-min incubation at 37 °C with shaking. One microliter of each sample was injected with a 4:1 split for tuber samples and a 10:1 split for leaf samples on an Agilent 7890B GC equipped with an Agilent 5977B MSD (Agilent Technologies, Santa Clara, CA, USA). The sample injection order was randomized, and the reagent blank was injected after every three samples to control for potential carryover. Resulting spectra were analyzed using AMDIS[25] and the Agilent Fiehn 2013 GC/MS Metabolomics RTL Library[26] to identify components.

Targeted metabolite analysis using High-Performance Liquid Chromatography (HPLC)

For HPLC analysis, 100 mg of ground, freeze-dried tuber tissue was extracted in 1 mL of a 50% methanol, 2.5% metaphosphoric acid, 1 mM EDTA extraction solution. Samples were shaken for 10 minutes at room temperature in the dark, then centrifuged at 14,000 × g for 10 min. Supernatant was moved to a new tube and re-centrifuged to remove debris. The supernatant was transferred to amber HPLC vials for injection. Metabolites were analyzed using standardized methods as previously published[27]. Standards were prepared in two combination sets: phenolic compounds (ascorbic acid, chlorogenic acid, tyrosine, tryptophan, and phenylalanine) and glycoalkaloids (solanine and chaconine). Phenolic compound standards were prepared with a seven-step 2x serial dilution ranging from 400 to 6.125 mg L^{-1}. Serial dilutions of glycoalkaloid standards were prepared at 400, 300, 200, 100, 50, 25, 12.5, and 6.125 mg L^{-1}. Each standard was injected in triplicate to generate standard curves used to calculate the compound concentrations in each sample. Compounds were analyzed using an UltiMate 3000 UHPLC system (Thermo Fisher Scientific, Waltham, MA, USA) with an LPG-3400SD quaternary analytical pump, solvent degasser, WPS-3000TSL autosampler, and TCC-3000 column compartment. Metabolites were separated using an Acclaim Polar Advantage II C18 column (4.6 × 150 mm, 5 µm) (Dionex, Sunnyvale, CA, USA) using previously published methods[27,28]. Compounds were detected by UV absorbance using a diode array detector DAD 3000 (Thermo Fisher Scientific).

RNA sequencing

Total RNAs were extracted from leaf samples collected as described above using a PureLink RNA mini kit (Invitrogen, Waltham, MA, USA), followed by treatment with DNase I (DNA-*free* DNA removal kit (Invitrogen)) to remove traces of genomic DNA. RNA integrity was

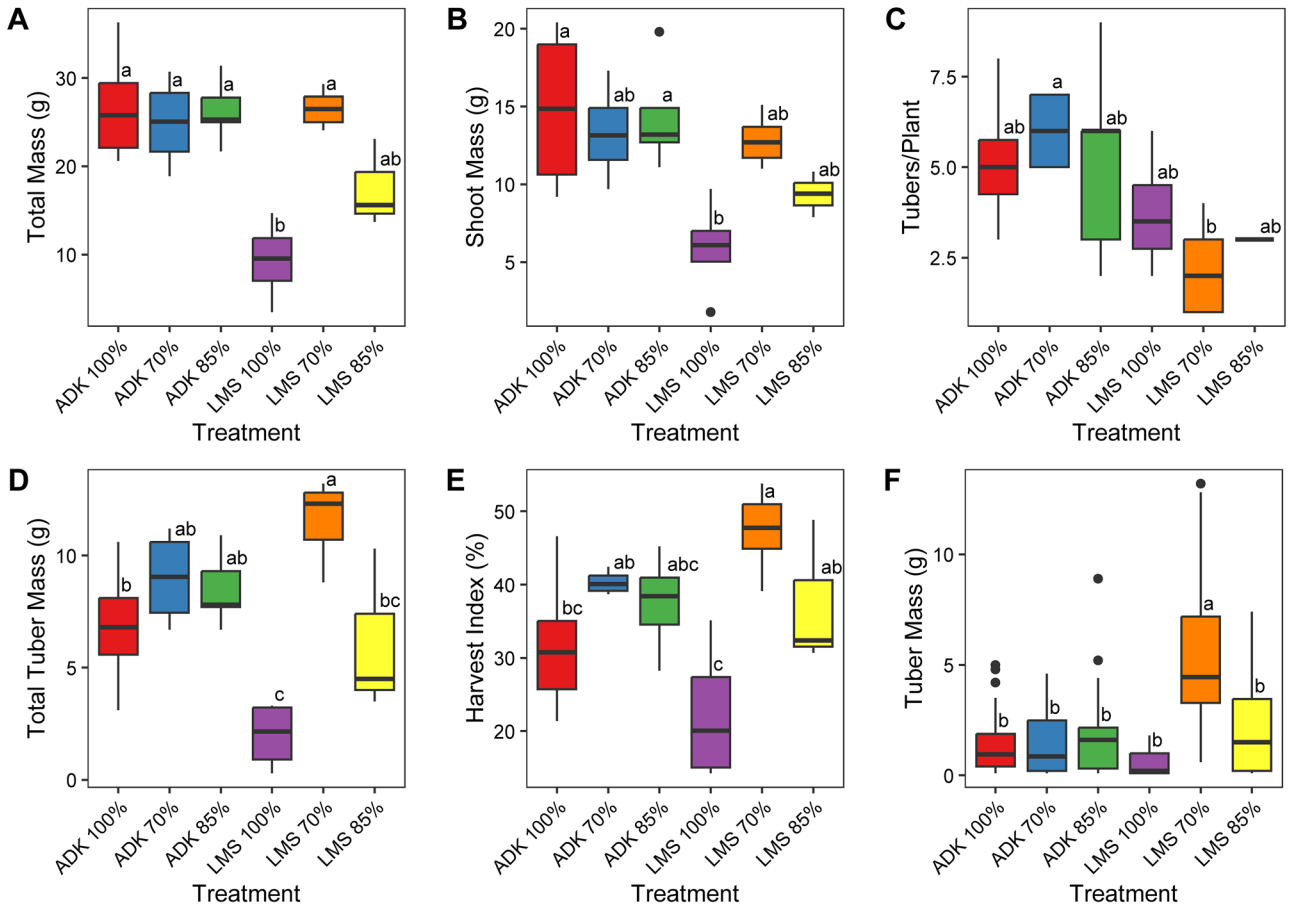


Fig. 1 | Harvest phenotypes of potato plant variety Modoc grown in variable ratios of LMS-1E and compost. **A** Total biomass, **B** Shoot biomass, **C** Tuber number, **D** Total tuber mass, **E** Harvest index, and **F** Average tuber mass. Shared letters indicate statistically similar groupings as determined by one-way ANOVA and Tukey's tests.

verified on agarose gel and by analysis on an Agilent Bioanalyzer 2100 (Agilent Technologies). RNAs were then sent to Novogene for sequencing on an Illumina Novaseq X Plus Series (150-bp, paired-ends) as previously described[29]. Raw fastq files were run through cutadapt to remove adapter sequences. The DM v6.1 doubled monoploid potato genome and Gene Ontology (GO) term annotations were downloaded from spuddb.uga.edu[30]. Reads were aligned to the genome using HISAT2[31], sorted using SAMtools[32], and mapped using STRINGTIE[33]. Gene counts were then analyzed in R using the DESeq2 package to generate lists of differentially expressed genes (DEGs), principal component analysis (PCA) plots, and heatmaps[34]. Replicate A of the OPRH4W30 treatment was removed as an outlier based on PCA clustering. Gene set enrichment analysis (GSEA) was performed using the ClusterProfiler package in R[35,36] and used to generate dot plots. GSEA serves to provide context to the genes being differentially expressed by sorting them by ontological categories and reporting them by biological function/pathway. The enriched pathways containing differentially expressed genes are then represented on dotplots.

Statistical analysis

In Experiment 1, because of unequal number of replicates per group, normality of residuals and homogeneity of variance were verified using Shapiro-Wilk test and Levene's test, respectively. Statistical analyses of GC-MS data were performed using MetaboAnalyst 6.0 using default processing settings and data filtering and using the reference feature ribitol for normalization[37]. Features with missing values across replicates were excluded, and a 5% low-variance filter was applied based on the interquantile range. Principle component analyses were generated based on these settings. For other data including harvest metrics, LCMS measurements, PlantEye600 data, and MultispeQ measurements, data were analyzed via ANOVA in R using the "dplyr" and "multcompview" packages[38,39]. Figures were generated using the "ggplot2", "RColorBrewer", and "ggpubr" packages[40–42].

Results

Determination of optimal LRS/compost ratio for potato growth (Experiment 1)

No statistically significant differences in canopy growth or physiology were detected during early development (Table S2 and Data S1), likely reflecting asynchronous emergence and associated within-treatment variation. By harvest, growth had stabilized within treatments and significant differences were observed across multiple phenotypes (Fig. 1). Plants grown in 100% LMS-1E showed the greatest reduction in total, shoot, root, and tuber biomass and harvest index relative to Adkins soil (Figs. 1 and 2, Data S2). Root development was most severely affected, with roots from three of four plants falling below the minimum detectable mass (<0.01 g). Plants in 70% LMS-1E were significantly larger than pure regolith control plants across all biomass metrics and comparable to Adkins soil plants in most phenotypes, with tuber mass matching or exceeding the terrestrial control in some replicates (Fig. 1F). Plants in 85% LMS-1E produced intermediate biomass, with no statistically significant difference from either the pure regolith control or Adkins soil. Compost amendment level had no significant effect on any phenotype in the Adkins soil series. Isolated significant differences in photosynthetic parameters were detected by MultispeQ but did not form consistent patterns across related traits (Table S3 and Data S3).

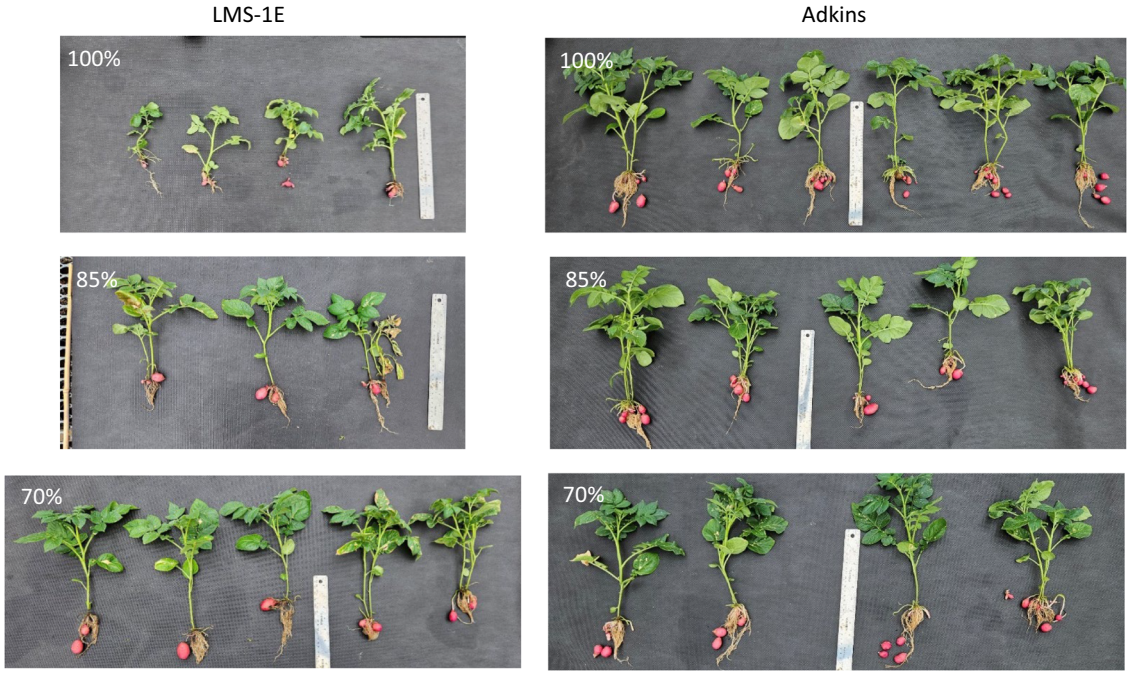


Fig. 2 | Growth and development phenotype of potato plants grown in LMS-1E and Adkins soil with or without amendment with vermicompost. Post-harvest images of potato plants grown in LMS-1E (left) and Adkins soil (right), in 100%, 85%, or 70% regolith to compost volume ratios.

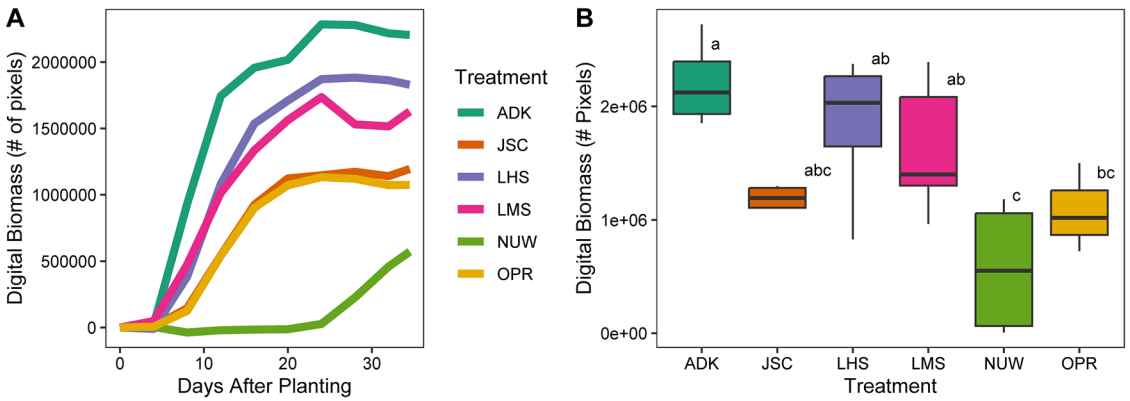


Fig. 3 | Digital above-ground biomass of potato plants grown in different lunar regolith simulants and Adkins Earth control. A Digital above-ground biomass across the first 34 days after planting (DAP) of potato plants grown in Adkins soil (ADK) and five regolith simulants; JSC-1A (JSC), LHS-1E (LHS), LMS-1E (LMS), NUW-LHT-5M (NUW), and OPRH4W30 (OPR). Data were collected via the Phenospex PlantEye600 scanner. **B** Boxplot of final above-ground digital biomass at 34 DAP. All substrates were amended with 5% compost by volume. Shared letters indicate statistically similar groupings determined by ANOVA followed by Tukey's post-hoc. $N = 5$ except NUW-LHT-5M where $N = 3$.

Heavy metal content in leaf and tuber tissues was quantified to investigate factors potentially contributing to growth impairment in the pure regolith control (Table S4). Root tissue was excluded given the near-complete absence of roots in 100% LMS-1E plants, and biological replicates were pooled within treatments for this analysis. Copper concentration in leaves was markedly elevated in 100% LMS-1E plants relative to all other treatments, with a lesser increase observed in tubers (Table S4). Total nutrient analysis indicated copper concentrations of 18 mg kg^{-1} in unamended LMS-1E (Table S5), increasing to 24.5 mg kg^{-1} pre-growth and 28 mg kg^{-1} post-growth following Osmocote addition (Table S6). Bioavailable copper concentrations, determined by Mehlich-3 extraction, were considerably lower (Table S5).

Pre-growth pH of 100% LMS-1E was 7.9, declining progressively with increasing vermicompost content, consistent with the near-neutral pH range of vermicompost (6–7; Table S6). Higher compost ratios corresponded with increased EC, microbial respiration, and detectable concentrations of several heavy metals, including Cu, Ni, and Zn. Post-growth, pH declined, and EC increased across all treatments relative to pre-growth values, consistent with plant-driven cation uptake. Post-growth concentrations of Al, Cr, Cu, Fe, Ni, and Zn were elevated relative to pre-growth levels based on nitric acid digestion. Microbial respiration declined post-growth in 85% and 70% LMS-1E treatments, while a marginal increase was observed in the pure regolith control.

Effect of various lunar regolith simulant types on potato growth (Experiment 2)

The growth of potato plants varies depending on the type of LRS. Plants grown in lunar highland simulant NUW-LHT-5M showed the most severe growth impairment, with statistically significant reductions in canopy size and tuber biomass relative to all other treatments (Fig. 3).

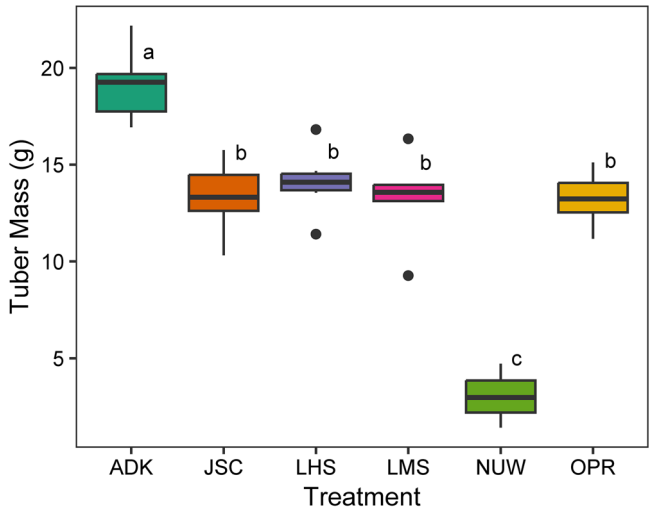


Fig. 4 | Tuber biomass of potato plants grown in different lunar regolith simulants and Adkins Earth control. Tubers were harvested at 59 DAP from plants grown in Adkins soil (ADK) and five regolith simulants; JSC-1A (JSC), LHS-1E (LHS), LMS-1E (LMS), NUW-LHT-5M (NUW), and OPRH4W30 (OPR). Shared letters indicate statistically similar groupings determined by ANOVA followed by Tukey's post-hoc. $N = 5$ except NUW-LHT-5M where $N = 3$.

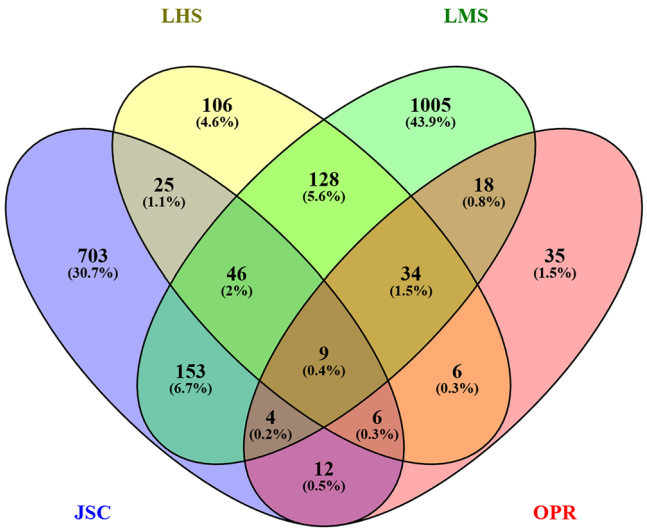


Fig. 5 | Number of differentially expressed genes in leaves of potato plants grown in four different lunar regolith simulants compared to Adkins Earth control. Venn diagram of differentially expressed genes ($p_{adj} < 0.05$) of plants grown in LHS-1E (LHS), LMS-1E (LMS), JSC-1A (JSC), and OPRH4W30 (OPR) compared with the terrestrial soil Adkins.

Emergence in NUW-LHT-5M was markedly delayed at approximately 24 DAP compared to 4–8 DAP across the remaining four LRS types (LHS-1E, OPRH4W30, JSC-1A, and LMS-1E), and only three of five plants attained sufficient size for scanner detection and produced harvestable tubers (Data S4 and Table S7). Tuber mass was significantly reduced in all five LRS types relative to Adkins soil (Fig. 4). Of the remaining simulants, canopy biomass was significantly reduced relative to Adkins soil only in lunar highland simulant OPRH4W30, while JSC-1A, LHS-1E, and LMS-1E did not differ significantly from Adkins soil in this metric (Fig. 3). No statistically significant differences in colorimetric indices were detected across any of the six treatments (Data S4).

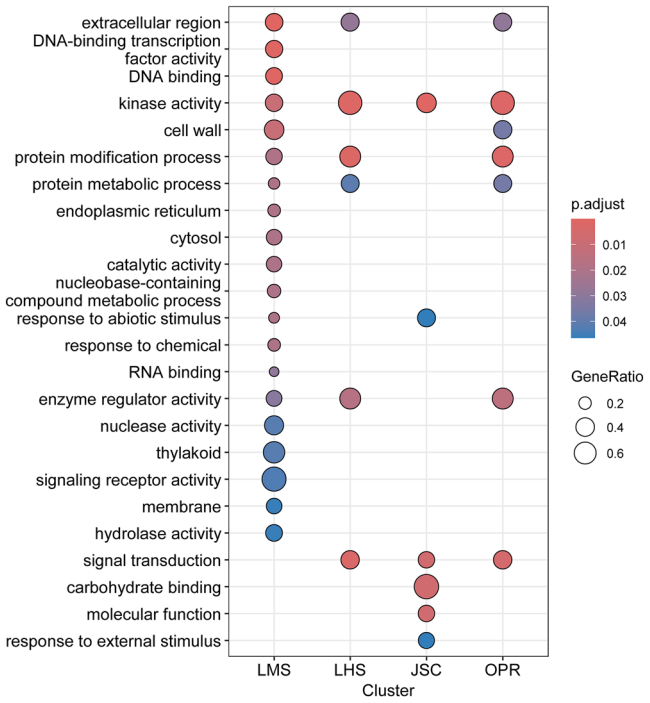


Fig. 6 | Gene Set Enrichment Analysis (GSEA) of differentially expressed genes between Adkins soil treatment and LRS. LMS-1E (LMS), LHS-1E (LHS), JSC-1A (JSC), OPRH4W30 (OPR). Dotplots display the gene ratio (count of enriched genes/count of total genes in pathway) of various GO terms based on comparison to Adkins control soil.

The potato leaf transcriptional and metabolic response differs between LRSs. RNA-seq analysis of leaves harvested from plants grown in JSC-1A, LMS-1E, OPRH4W30, LHS-1E, and Adkins soil yielded a total of 972,140,076 raw reads (Table S8). Differential gene expression analysis relative to Adkins soil revealed varying numbers of DEGs (p adj < 0.05) across LRS types (Fig. 5 and Data S5). The fewest DEGs were identified in OPRH4W30 (124 genes), while LMS-1E, JSC-1A, and LHS-1E produced 1397, 958, and 360 DEGs, respectively. DEGs in JSC-1A and LMS-1E were largely unique to each simulant, whereas the majority of DEGs in LHS-1E were shared with those identified in LMS-1E (Fig. 5). Gene set enrichment analysis revealed enrichment of 20, 7, 6, and 6 GO terms (p adj < 0.05) in LMS-1E, OPRH4W30, JSC-1A, and LHS-1E, respectively, relative to Adkins soil (Fig. 6 and Data S6). Kinase activity (GO:0016301) was the only GO term enriched across all four LRS types, while the broader pattern of enriched terms was simulant-specific.

GC-MS metabolite profiling of leaf tissue revealed distinct metabolic profiles in LRS-grown plants relative to Adkins soil controls (Fig. 7 and Data S7), with sucrose, fructose, and citric acid among the primary contributors to treatment separation (Fig. 7).

Taken together, transcriptomic and metabolomic profiles differed across LRS types, indicating that individual simulants generate distinct stress signatures in potato leaves.

Tuber metabolites and nutrients levels in LRS are similar to those found in Adkins. GC-MS analysis of tuber metabolites revealed only minor changes between treatments (Fig. 8 and Data S8). In addition, analysis of phenolic compounds and two major glycoalkaloids, solanine and chaconine, via HPLC-UV/VIS did not reveal significant changes in 6 out of 7 compounds analyzed (Fig. 9). Tyrosine concentrations increased significantly in plants grown in lunar mare simulant JSC-1A compared to Adkins but did not increase significantly in lunar mare simulant LMS-1E and lunar highland simulants LHS-1E and OPRH4W30. Heavy metal

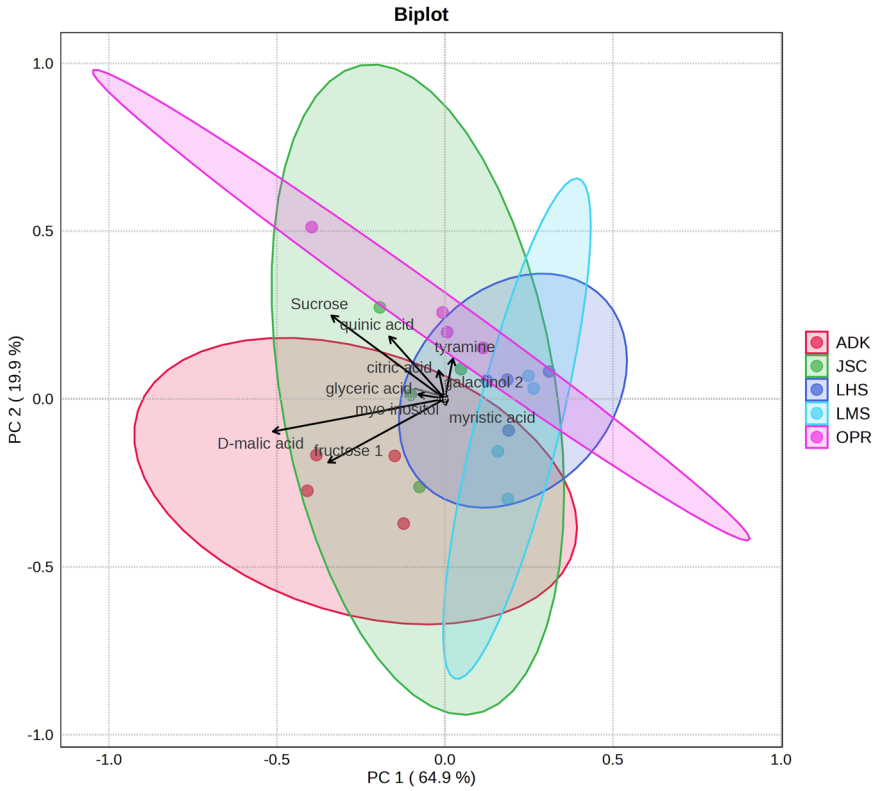


Fig. 7 | PCA biplot of GC-MS metabolite analysis of leaves collected at 39 DAP from potato plants grown in Adkins soil (ADK) and four lunar regolith simulants. JSC-1A (JSC), LHS-1E (LHS), LMS-1E (LMS), and OPRH4W30 (OPR).

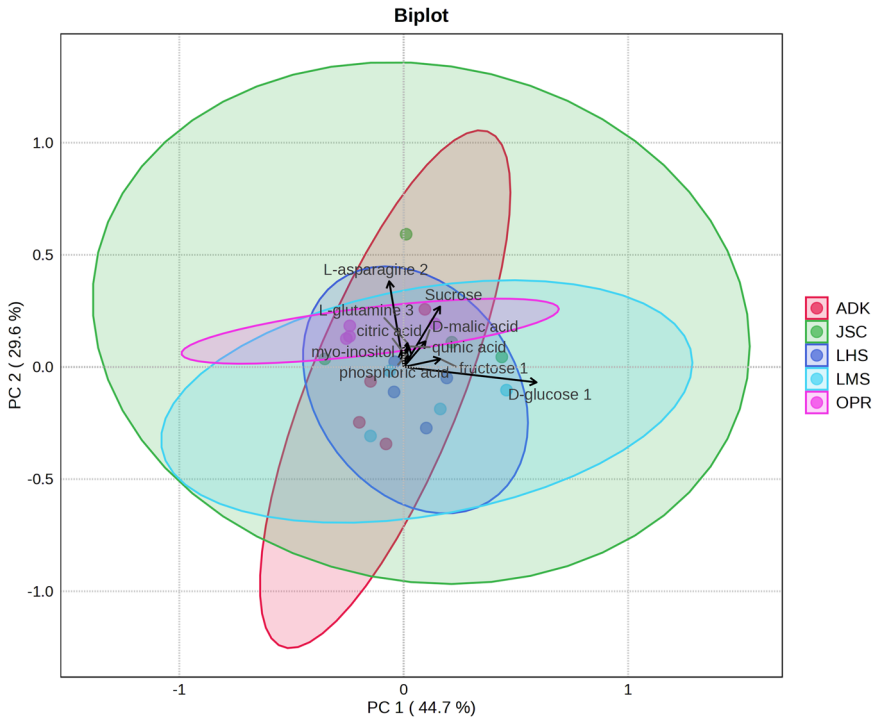


Fig. 8 | PCA biplot of GC-MS metabolite analysis of tubers harvested at 59 DAP from potato plants grown in Adkins soil (ADK) and four lunar regolith simulants. JSC-1A (JSC), LHS-1E (LHS), LMS-1E (LMS), and OPRH4W30 (OPR).

analysis of tubers revealed increased accumulation of Cu in JSC-1A and Zn in JSC-1A, LMS-1E, and OPRH4W30. Increased accumulation of Al in tubers grown in lunar highland simulants LHS-1E and OPRH4W30 was also observed (Tables 1 and S9). Overall, our data indicate that tubers' nutritional profiles are unique to each type of LRS but are only mildly affected compared to Adkins control.

Differences in soil characteristics that may explain differential phenotypic response. Soil analysis revealed several differences between LRSs and Adkins soil (Table 2 or Data S9). All LRSs had higher moisture content, indicating reduced drainage capability (Table 2). Post-growth, the lunar mare simulants LMS1-E and JSC-1A and lunar highland simulant LHS1-E all had a reduction in pH from 7.5 to

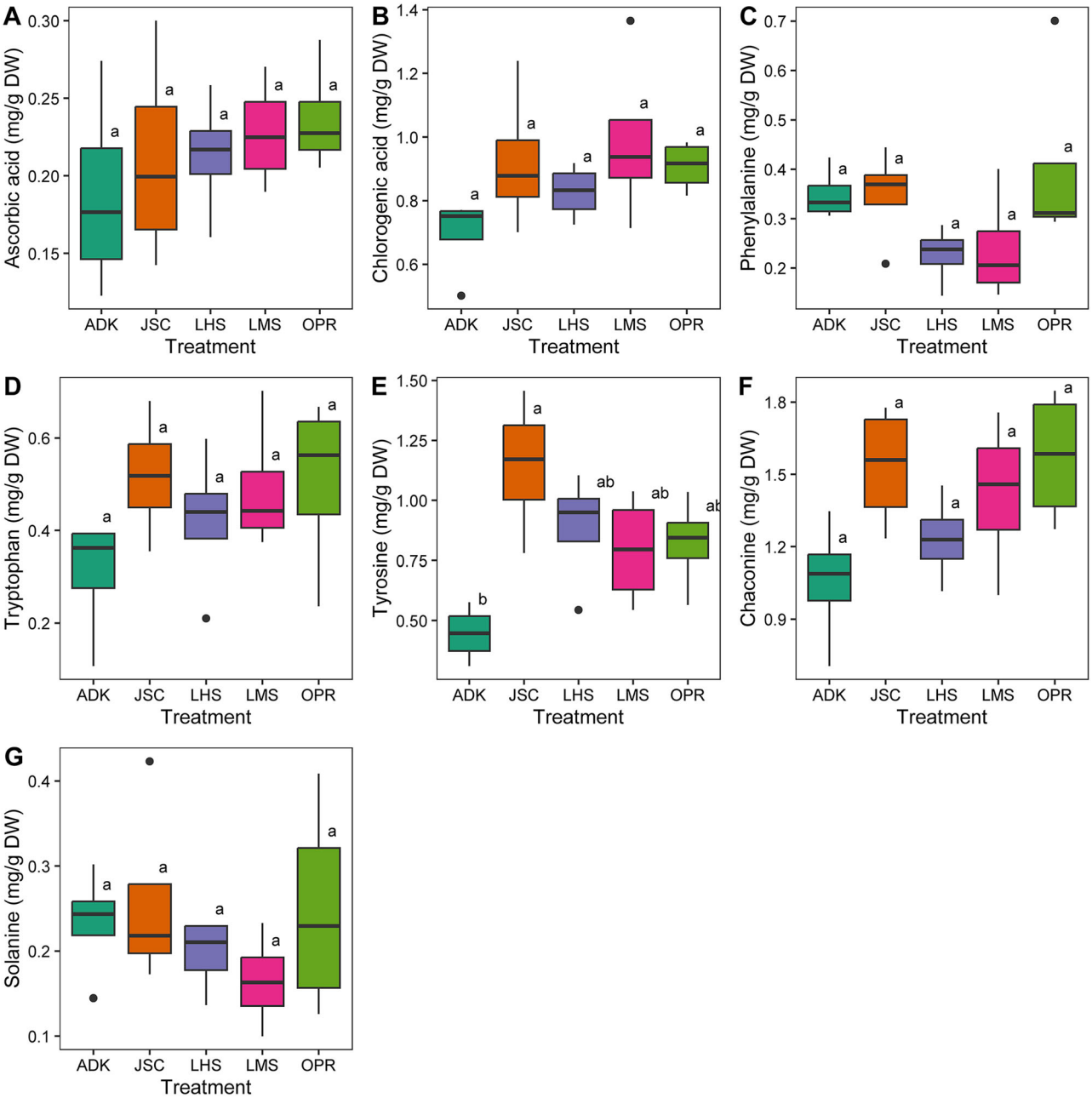


Fig. 9 | Quantities of targeted compounds extracted from harvested tubers of potato plants grown in Adkins soil (ADK) and four lunar regolith simulants. JSC-1A (JSC), LHS-1E (LHS), LMS-1E (LMS), and OPRH4W30 (OPR). **A** Ascorbic acid, **B** chlorogenic acid, **C** phenylalanine, **D** tryptophan, **E** tyrosine, **F** chaconine, and **G** solanine. Shared letters indicate statistically similar groupings determined by ANOVA followed by Tukey's post-hoc.

7.72 range to ~6.5, whereas lunar highland simulant OPRH4W30 remained at ~7.5, compared to pre-growth samples (Table S10). Electroconductivity increased in all LRSs compared to pre-growth samples (Tables 2 and S10). Elemental availability was also altered in all LRS for some elements, such as Ca, K, Mg, and Zn, between pre- and post-growth samples (Tables 2 and S10). However, this is consistent with changes in pH, which determines the solubility of many elements.

Discussion

In this study, we tested potato growth on LRS with or without organic matter amendment, tested whether potato responds similarly or differently to a variety of LRS types, and characterized the potato response to LRS at the molecular level. Because LRSs do not contain any nitrogen and contain limiting quantities of the other macronutrients potassium and phosphorous

Table 1 | Heavy metal content of tubers grown in various LRS with 5% v/v vermicompost, determined by ICP-OES

Soil type	Heavy metal content (mg kg^{-1} dry weight)		
	Al	Cu	Zn
ADK	55.9 ± 3.03^{b}	2.8 ± 0.32^{b}	6.6 ± 0.31^{b}
JSC	59.3 ± 6.42^{b}	6.0 ± 0.60^{a}	12.3 ± 1.08^{a}
LHS	144.6 ± 11.60^{a}	4.7 ± 1.08^{ab}	9.5 ± 0.63^{ab}
LMS	50.8 ± 3.74^{b}	5.1 ± 0.00^{ab}	11.4 ± 0.51^{a}
OPR	185.1 ± 26.88^{a}	6.0 ± 0.32^{ab}	12.0 ± 0.64^{a}

Letters indicate statistically similar groupings determined by one-way ANOVA and Tukey's post-hoc, performed in R. $N = 4$. As, Cd, Co, Cr, Ni, Pb were also analyzed but found below quantifiable levels in all samples.

Table 2 | Post-growth soil characteristics of soil substrates amended with 5% (v/v) vermicompost

	Moisture (%)	pH	EC (dS m^{-1})	Elemental quantities (mg kg^{-1})									Microbial respiration (µg CO_2-C g^{-1} dry soil day^{-1})		Organic matter (%)
				Al	Ca	Cu	Fe	K	Mg	Mn	P	Zn	24 h	96 h	
ADK	7.70 ± 0.90^{b}	6.38 ± 0.10^{b}	0.51 ± 0.09^{a}	464.24 ± 9.64^{e}	1578.67 ± 29.92^{b}	2.70 ± 0.29^{bc}	115.76 ± 5.06^{e}	221.24 ± 13.92^{ab}	229.49 ± 6.03^{c}	31.88 ± 0.54^{c}	56.83 ± 4.97^{b}	2.00 ± 0.29^{b}	5.56 ± 0.25^{a}	2.26 ± 0.23^{b}	1.13 ± 0.03^{a}
JSC	11.63 ± 2.07^{ab}	6.69 ± 0.16^{b}	0.85 ± 0.10^{a}	1161.58 ± 30.19^{b}	1666.09 ± 45.28^{b}	2.70 ± 0.15^{bc}	1526.69 ± 37.23^{b}	268.39 ± 22.28^{a}	567.91 ± 15.34^{a}	38.59 ± 1.01^{b}	29.21 ± 2.02^{c}	4.50 ± 0.35^{b}	5.14 ± 0.11^{a}	2.45 ± 0.11^{b}	0.52 ± 0.03^{c}
LHS	12.60 ± 1.39^{ab}	6.52 ± 0.04^{b}	0.74 ± 0.05^{a}	866.32 ± 11.59^{c}	1567.52 ± 33.05^{b}	1.66 ± 0.20^{c}	417 ± 12.34^{d}	177.23 ± 12.13^{bc}	135.91 ± 5.06^{d}	10.42 ± 0.23^{e}	66.88 ± 3.25^{ab}	4.21 ± 0.30^{b}	6.30 ± 0.38^{a}	3.27 ± 0.27^{ab}	0.58 ± 0.03^{c}
LMS	17.06 ± 3.14^{ab}	6.46 ± 0.11^{b}	0.94 ± 0.14^{a}	664.90 ± 30.36^{d}	1210.03 ± 60.24^{c}	3.34 ± 0.24^{ab}	1066.22 ± 38.93^{c}	203.57 ± 20.36^{abc}	368.12 ± 20.74^{b}	24.32 ± 1.01^{d}	83.94 ± 4.55^{b}	4.83 ± 0.76^{b}	6.37 ± 0.63^{a}	3.49 ± 0.25^{a}	0.61 ± 0.03^{c}
OPR	19.75 ± 0.53^{a}	7.53 ± 0.05^{a}	0.95 ± 0.07^{a}	1337.32 ± 13.10^{a}	7035.16 ± 87.10^{a}	4.09 ± 0.13^{a}	1924.68 ± 26.19^{a}	138.20 ± 8.83^{c}	203.55 ± 3.27^{c}	43.36 ± 0.70^{a}	23.18 ± 1.27^{c}	10.05 ± 1.70^{a}	6.10 ± 0.43^{a}	2.62 ± 0.26^{ab}	0.85 ± 0.03^{b}

Data are means ± SE (N = 4). Identical letters in superscript indicate statistically similar groupings according to ANOVA followed by Tukey's post-hoc. Analysis was performed in R.

and possibly some micronutrients, we provided plants with the slow-release fertilizer Osmocote as a complete source of nutrients. This enabled us to eliminate the confounding effect of nutrients deficiencies and to characterize the response of potato to LRS exposure.

Growth was severely affected when potato plants were grown in 100% lunar simulant LMS-1E. Symptoms included stunting and underdeveloped roots. These symptoms are typical of plants with excess copper[43,44]. Interestingly, leaf and tuber tissues of plants grown in 100% LMS-1E accumulated higher copper levels compared to Adkins control (Table S4), which is indirect evidence of copper accumulation in roots, as copper is poorly mobile in the vascular tissues and roots are known to accumulate much higher concentrations of copper than shoots[43]. The negative effect of 100% LMS-1E was alleviated by adding compost to the growth substrate (Fig. 1). We hypothesize that the addition of organic matter provides additional binding sites for copper[45], thereby decreasing bioavailability and alleviating hyperaccumulation of copper in plant tissues. Recently, it was reported that *Arabidopsis thaliana* plants grown in genuine lunar regolith and simulants were stunted, had short roots, and abbreviated growth and arrest in the vegetative stages[46]. These phenotypes were, at least in part, due to oxidative damage of the genome. Interestingly, pre-wash of LRS with antioxidant cocktail, particularly glutathione[47], improved genome oxidation of plants grown in LRS and enabled plants to transition from the vegetative to the reproductive stage[47]. Given that glutathione is a chelator of copper and other heavy metals, our results and previous ones suggest that managing heavy metals present in LRS will be essential for successfully growing crops in lunar regolith.

Potato plants grown in different lunar mare and lunar highland regolith simulants amended with 5% vermicompost were able to complete a full life cycle, developed roots, and produced tubers. However, they were all negatively affected in canopy size and tuber yield compared to those grown in Adkins, showing that LRS remained a stressful environment under these compost amendment conditions. In addition to the potential toxicity of heavy metals mentioned above, the presence of glassy agglutinates in lunar highland simulants OPRH4W30 and NUW-LHT-5M may be particularly problematic for plant growth[17,48], though work verifying this is limited due to difficulty simulating agglutinates. As such, more work is needed to specifically study the effects of agglutinates on plant growth. Lunar mare simulant JSC-1A, despite lacking in agglutinates, does contain a high glass fraction[49] and caused similar issues as OPRH4W30. These sharp micro-particles may cause abrasions on root/stolon/tuber epidermis. However, we have not investigated this hypothesis. High levels of compaction and cementation of lunar highland simulant NUW-LHT-5M and lunar mare simulant JSC-1A after watering might also have negatively affected plant growth and development. This is consistent with the higher moisture content recorded in LRSs versus the Adkins soil. Finally, it is likely that all together these factors caused the stunting observed. Potato plants responded to this stressful environment by modifying the expression of genes involved in stress responses and signaling. Interestingly, each regolith simulant induced unique gene expression changes. This uniqueness was also observed in *A. thaliana* in response to lunar regolith returned from three Apollo sites[46]. These results indicate that the specific stress generated by regolith and its simulants varies depending on the type of lunar regolith or LRS.

Although the focus of current studies is to test the ability of different plant species to produce food biomass, it is essential to ensure that the food produced is edible. Our data showed that growth in LRS did not significantly alter potato tuber metabolite profiles, indicating negligible changes to nutritional content. Importantly, stress induced by LRS did not cause statistically significant increases in the main potato glycoalkaloid levels, solanine and chaconine. Heavy metal analysis revealed mild accumulation of Zn and Cu in tubers grown in LRS. In addition, plants grown in highland-type LRS were found to accumulate aluminum, which is not of immediate concern for human consumption purposes, but could contribute to long-term negative impacts on plant

production. These findings support that tuber nutritional quality is maintained in LRS-grown tubers. This will need to be verified in future experiments.

Finally, it is important to remember that LRSs have several limitations that distinguish them from genuine lunar regolith. A recent report in *A. thaliana* showed that there were major differences in the plant response to JSC-1A, a terrestrial LRS, and Apollo lunar regolith[46], illustrating that results obtained in experiments done in LRS must be considered cautiously.

In conclusion, these findings demonstrate that potato can complete its full life cycle and produce harvestable tubers in lunar regolith simulants when supplemented with vermicompost, supporting the feasibility of regolith-based crop production for lunar bioregenerative life support systems. Notably, incorporation of as little as 30% vermicompost was sufficient to restore plant biomass and morphology to levels comparable to a terrestrial soil control, establishing organic matter amendment as a practical and scalable remediation strategy for early-stage lunar agriculture. Growth impairment and stress intensity varied markedly across the five LRS types tested, and transcriptomic profiling revealed that each simulant elicited a distinct molecular stress signature in potato leaves, demonstrating that regolith composition drives qualitatively different plant stress responses rather than a generalized reaction to an inhospitable substrate. Despite this pronounced transcriptional reprogramming, tuber metabolite profiles including glycoalkaloid levels remained largely unaltered relative to controls, and heavy metal accumulation in tuber tissue was modest. This is the first report to simultaneously characterize growth, transcriptomic, and metabolomic responses of potato to multiple LRS types, and the first to provide evidence that tubers produced in lunar regolith simulants are nutritionally comparable to those grown in terrestrial soil, a critical step toward validating lunar food production for long-duration human exploration.

Data availability

The raw sequence reads have been deposited in the Open Science Data Repository under https://doi.org/10.26030/w56j-2d69.

Received: 24 February 2026; Accepted: 17 October 2026;
Published online: 19 November 2026

References

1. *A New Era in Space*. https://doi.org/10.17226/27792 (National Academies Press, 2024).
2. Ming, D. W. & Henninger, D. L. Use of lunar regolith as a substrate for plant growth. *Adv. Sp. Res.* **14**, 435–443 https://doi.org/10.1016/0273-1177(94)90333-6 (1994).
3. Taylor, S. R. The Moon. *Encycl. Sol. Syst.* 227–250 https://doi.org/10.1016/B978-012088589-3/50016-5 (2007).
4. Duri, L. G. et al. The potential for lunar and Martian regolith simulants to sustain plant growth: a multidisciplinary overview. *Front. Astron. Sp. Sci.* **8**, https://doi.org/10.3389/fspas.2021.747821 (2022).
5. Fackrell, L. E., Humphrey, S., Loureiro, R., Palmer, A. G. & Long-Fox, J. Overview and recommendations for research on plants and microbes in regolith-based agriculture. *Npj Sustain. Agric.* **2**, 15 https://doi.org/10.1038/s44264-024-00013-5 (2024).
6. Madison, A. et al. Lunar dust simulants and their applications. 86–94. https://doi.org/10.1061/9780784484470.008 (2023).
7. Caporale, A. G. et al. Green compost amendment improves potato plant performance on Mars regolith simulant as substrate for cultivation in space. *Plant Soil* **486**, 217–233 https://doi.org/10.1007/s11104-022-05860-0 (2023).
8. El Kamouh, A., El Chami, D., Abdelmouneim, A. A., Khadra, R. & De Pascale, S. A systematic review of plant cultivation and growth in extraterrestrial regolith simulants. *Life Sci. Sp. Res.* https://doi.org/10.1016/j.lssr.2026.04.005 (2026).
9. Walkinshaw, C. H., Sweet, H. C., Venketeswaran, S. & Horne, W. H. Results of Apollo 11 and 12 quarantine studies on plants. *Bioscience* **20**, 1297–1302 https://doi.org/10.2307/1295365 (1970).
10. Walkinshaw, C. H. & Johnson, P. H. Analysis of vegetable seedlings grown in contact with Apollo 14 lunar surface Fines1. *HortScience* **6**, 532–535 https://doi.org/10.21273/HORTSCI.6.6.532 (1971).
11. Wamelink, G. W. W., Frissel, J. Y., Krijnen, W. H. J. & Verwoert, M. R. Crop growth and viability of seeds on Mars and Moon soil simulants. *Open Agric.* **4**, 509–516 https://doi.org/10.1515/opag-2019-0051 (2019).
12. Duri, L. G. et al. Mars regolith simulant ameliorated by compost as in situ cultivation substrate improves lettuce growth and nutritional aspects. *Plants* **9**, 628 https://doi.org/10.3390/plants9050628 (2020).
13. Caporale, A. G. et al. Geo-mineralogical characterisation of Mars simulant MMS-1 and appraisal of substrate physico-chemical properties and crop performance obtained with variable green compost amendment rates. *Sci. Total Environ.* **720**, 137543 https://doi.org/10.1016/j.scitotenv.2020.137543 (2020).
14. Jemison Jr, J. M., Sexton, P. & Camire, M. E. Factors influencing consumer preference of fresh potato varieties in Maine. *Am. J. Potato Res.* **85**, 140–149 https://doi.org/10.1007/s12230-008-9017-3 (2008).
15. Kovtun, R. An overview of lunar regolith simulants. https://ntrs.nasa.gov/api/citations/20230016971/downloads/Simulant. Characterization Talk LSIC.pdf (2023).
16. Ray, C. S., Reis, S. T., Sen, S. & O'Dell, J. S. JSC-1A lunar soil simulant: Characterization, glass formation, and selected glass properties. *J. Non Cryst. Solids* **356**, 2369–2374 https://doi.org/10.1016/j.jnoncrysol.2010.04.049 (2010).
17. Rickman, D. L. et al. Characterization of NUW-LHT-5M, a lunar highland simulant. http://www.sti.nasa.gov. (2024).
18. Lunar Highland Simulant (LHS-1E) datasheet. https://cdn.shopify.com/s/files/1/0398/9268/0862/files/lhs-1E-spec-sheet-Dec2023.pptx_ee9576ee-98f2-4e1b-ba2d-7dff30cedba9.pdf?v=1756996302 (2023).
19. Lunar Mare Simulant (LMS-1E) datasheet. https://cdn.shopify.com/s/files/1/0398/9268/0862/files/LMS-1E-SPEC-SHEET-DEC2025.pptx.pdf?v=1764081546 (2023).
20. Thiamin addition to soil increases potato tuber thiamin content under greenhouse conditions. *PeerJ* 1–23. https://doi.org/10.7717/peerj.20684 (2026).
21. *Interpreting Compost Analyses*. https://catalog.extension.oregonstate.edu/sites/catalog/files/project/pdf/em9217.pdf (Oregon State University Extension Service, 2018).
22. Johnson, S. B. *Phosphorus: An Essential Element*, 1–3 (University of Maine Cooperative Extension, 2020).
23. Hill, E., Mellin, M. J., Deane, B., Liu, Y., & Taylor, L. A. Apollo sample 70051 and high- and low-Ti lunar soil simulants MLS-1A and JSC-1A: implications for future lunar exploration, *J. Geophys. Res. Planets* **112**, https://doi.org/10.1029/2006JE002767 (2007).
24. Bvindi, C. et al. Potato non-specific lipid transfer protein StnsLTPI.33 is associated with the production of reactive oxygen species, plant growth, and susceptibility to *Alternaria solani*. *Plants* **12**, 3129 https://doi.org/10.3390/plants12173129 (2023).
25. Davies, T. The new automated mass spectrometry deconvolution and identification system (AMDIS). *Spectrosc. Eur.* **10**, 24–27 (1998).
26. Kind, T. et al. FiehnLib: mass spectral and retention index libraries for metabolomics based on quadrupole and time-of-flight gas chromatography/mass spectrometry. *Anal. Chem.* **81**, 10038–10048 https://doi.org/10.1021/ac9019522 (2009).
27. Goyer, A., Picard, M., Hellmann, H. A. & Mooney, S. L. Effect of low-temperature storage on the content of folate, vitamin B6, ascorbic acid, chlorogenic acid, tyrosine, and phenylalanine in potatoes. *J. Sci. Food Agric.* **99**, 4842–4848 https://doi.org/10.1002/jsfa.9750 (2019).
28. Torabian, S. et al. Effect of potassium fertilizer, genetic makeup, and environment on the potato tuber nutrition. *J. Agric. Food Res.* **19**, 101645 https://doi.org/10.1016/j.jafr.2025.101645 (2025).

29. Berrian, T. W. et al. Investigation of the effectiveness and molecular mechanisms of thiamin priming to control early blight disease in potato. *Phytopathol.®* **115**, 234–246 https://doi.org/10.1094/PHYTO-09-24-0277-R (2025).
30. Hamilton, J. P., Brose, J. & Buell, C. R. SpudDB: a database for accessing potato genomic data. *Genetics* **229**, 205 https://doi.org/10.1093/genetics/iyae205 (2025).
31. Kim, D., Paggi, J. M., Park, C., Bennett, C. & Salzberg, S. L. Graph-based genome alignment and genotyping with HISAT2 and HISAT-genotype. *Nat. Biotechnol.* **37**, 907–915 https://doi.org/10.1038/s41587-019-0201-4 (2019).
32. Li, H. et al. The Sequence Alignment/Map format and SAMtools. *Bioinformatics* **25**, 2078–2079 https://doi.org/10.1093/bioinformatics/btp352 (2009).
33. Pertea, M. et al. StringTie enables improved reconstruction of a transcriptome from RNA-seq reads. *Nat. Biotechnol.* **33**, 290–295 https://doi.org/10.1038/nbt.3122 (2015).
34. Love, M. I., Huber, W. & Anders, S. Moderated estimation of fold change and dispersion for RNA-seq data with DESeq2. *Genome Biol.* **15**, 550 https://doi.org/10.1186/s13059-014-0550-8 (2014).
35. Xu, S. et al. Using clusterProfiler to characterize multiomics data. *Nat. Protoc.* **19**, 3292–3320 https://doi.org/10.1038/s41596-024-01020-z (2024).
36. Yu, G. Thirteen years of clusterProfiler. *Innov* **5**, 100722 https://doi.org/10.1016/j.xinn.2024.100722 (2024).
37. Pang, Z. et al. MetaboAnalyst 6.0: towards a unified platform for metabolomics data processing, analysis and interpretation. *Nucleic Acids Res.* **52**, W398–W406 https://doi.org/10.1093/nar/gkae253 (2024).
38. Wickham, H., Francois, R., Henry, L., Muller, K., Vaughan, D. A Grammar of Data Manipulation, (2026). https://dplyr.tidyverse.org.
39. S. Graves, H.-P. Piepho, L. Selzer, S. Dorai-Raj, multcompView: Visualizations of Paired Comparisons, (2024). https://cran.r-project.org/package=multcompView.
40. H. Wickham, ggplot2, Springer International Publishing, Cham, 2016. https://doi.org/10.1007/978-3-319-24277-4.
41. E. Neuwirth, RColorBrewer: ColorBrewer Palettes, (2022). https://cran.r-project.org/package=RColorBrewer.
42. A. Kassambara, ggpubr: "ggplot2" Based Publication Ready Plots, (2025). https://cran.r-project.org/package=ggpubr.
43. A. Moore, M. Satterwhite, J. Ippolito, Soil copper thresholds for potato production, in: West. Nutr. Manag. Conf., 2013: 152–155.
44. Mir, A. R., Pichtel, J. & Hayat, S. Copper: uptake, toxicity and tolerance in plants and management of Cu-contaminated soil. *BioMetals* **34**, 737–759 https://doi.org/10.1007/s10534-021-00306-z (2021).
45. E. J. M. Temminghoff, S. E. A. T. M. Van der Zee, F. A. M. de Haan, Copper Mobility in a Copper-Contaminated Sandy Soil as Affected by pH and Solid and Dissolved Organic Matter, Environ. Sci. Technol. 31 (1997) 1109–1115. https://doi.org/10.1021/es9606236.
46. A.-L. Paul, S. M. Elardo, R. Ferl, Plants grown in Apollo lunar regolith present stress-associated transcriptomes that inform prospects for lunar exploration, Commun. Biol. 5 (2022) 382. https://doi.org/10.1038/s42003-022-03334-8.
47. Barcenilla, B. B. et al. Telomere dynamics and oxidative stress in Arabidopsis grown in lunar regolith simulant. *Front. Plant Sci.* **15**, 1351613, https://doi.org/10.3389/fpls.2024.1351613 (2024).
48. M. C. Roth V. G. Roux, L. Roux, MECHANICAL PROPERTIES OF LUNAR REGOLITH SIMULANTS, 2025.
49. Sen, S. et al. Production of high fidelity lunar agglutinate simulant. *Adv. Sp. Res.* **47**, 1912–1921 https://doi.org/10.1016/j.asr.2011.02.005 (2011).

Acknowledgements

We thank Matthew Barrow at CSS Farms for providing Modoc minitubers.

Author contributions

D.H.: design of the work, acquisition, analysis, and interpretation of data, wrote first draft of the manuscript; A.L.: data acquisition; M.K.: data acquisition; S.C.: data acquisition; P.J.: funding acquisition, design of the work, reviewed and edited the manuscript; J.C.A.: data acquisition, reviewed and edited the manuscript; A.G.: conception, funding acquisition, design of the work, analysis and interpretation of data, reviewed and edited the manuscript. All authors have approved the submitted manuscript.

Funding

This work was supported by NASA Grant 80NSSC24K0755 to A.G. and P.J. A.L. and S.C. were supported by funding from the Oregon State University URSA Engage program, and M.K. was supported by funding from the Oregon State University College of Agricultural Sciences Beginning Researcher Program.

Competing interests

The authors declare no competing interests.

Additional information

Supplementary information The online version contains supplementary material available at https://doi.org/10.1038/s41526-026-00668-z.

Correspondence and requests for materials should be addressed to Aymeric Goyer.

Reprints and permissions information is available at http://www.nature.com/reprints

Publisher's note Springer Nature remains neutral with regard to jurisdictional claims in published maps and institutional affiliations.

Open Access This article is licensed under a Creative Commons Attribution 4.0 International License, which permits use, sharing, adaptation, distribution and reproduction in any medium or format, as long as you give appropriate credit to the original author(s) and the source, provide a link to the Creative Commons licence, and indicate if changes were made. The images or other third party material in this article are included in the article's Creative Commons licence, unless indicated otherwise in a credit line to the material. If material is not included in the article's Creative Commons licence and your intended use is not permitted by statutory regulation or exceeds the permitted use, you will need to obtain permission directly from the copyright holder. To view a copy of this licence, visit http://creativecommons.org/licenses/by/4.0/.

© The Author(s) 2026